

Paraná River Delta 2013 flood monitoring using AMSR-2, SMOS, Aquarius and Cosmo Skymed data.

Salvia, M., Grings, F., Bruscantini, C., Barraza, V.,
Perna, P., Karszenbaum, H.
Instituto de Astronomía y Física del Espacio
(IAFE, CONICET-UBA)
Buenos Aires, Argentina
msalvia@iafe.uba.ar

Ferrazzoli, P.
Ingegneria, DISP
Tor Vergata University
ferrazzoli@disp.uniroma2.it

Abstract—This paper compares the performance of Aquarius, SMOS and AMSR2 data to estimate the fraction of flooded area and mean water level inside a wetland, in the framework of an active/passive flood monitoring algorithm. The method, which is an extension of previously developed algorithms based on passive data, exploits the synergy of passive and active microwave signatures and model simulations of vegetation emissivity. The procedure is applied to a moderate event that occurred on the Paraná River Delta in 2013. We discuss the effect that the different spatial resolutions have for this hydrological application.

Keywords— Active and passive microwave systems; flooded fraction; Aquarius; SMOS; AMSR2

I. INTRODUCTION

Flooding is of major concern in the Plata Basin. This multinational basin, covering 3.2 million km², comprises the de la Plata River and its main tributaries, the Paraguay, Paraná, and Uruguay rivers. This region is of significant social and economic importance because it is densely populated, and has important agricultural activities (this area, includes the Argentinean “Pampa Húmeda” and is one of the richest agricultural regions in South America). This hydrographic network serves a population of about 70 million providing irreplaceable ecological/hydrological functions, such as mitigating large floods and droughts, recharging aquifers, supporting fish breeding areas and supplying the majority of the high quality fresh water.

The largest flood of the century occurred on the Paraná River in 1983 during a strong ENSO event. For a year and a half after the event, the Paraná flood level was above street level in areas of Santa Fe, Argentina. Economic losses due to floods in Argentina during the 1983, 1992, 1998, 1998, 2007 and 2009-2010 episodes exceeded US\$1 billion each.

This means that providing information on the current state of the basin hydrologic system on a systematic basis is critical to the regional economies and society, since any improvement in monitoring or prediction will have significant societal benefits.

Over the past decade, several flood monitoring/forecasting methodologies based on remote sensing data have been proposed. Among them, the ones based on microwave

This work was funded by Project MinCyT-NASA-CONAE n°12: “La Plata Basin floods and droughts: Contribution of microwave remote sensing in monitoring and prediction”.

observations are the most successful, since large flood events and intense cloud covers are often encountered simultaneously. This is a severe limitation of flood monitoring based on optical instruments.

In general, flooding increases the moisture of the soil and decreases its roughness. For higher water levels and in presence of vegetation cover, flooding also reduces the height of the emerged vegetation. In extreme cases, water level submerges vegetation. All these processes produce a decrease of the surface emissivity and an increase of the difference between the emissivity measured in the vertical and horizontal polarizations. Therefore, passive microwave polarization index (PI) has the potential to detect the fraction of inundated area and to monitor the increase of water level. These issues have been discussed in several papers [1] [2] [3]. Furthermore, the backscattering coefficient is also sensitive to flooding and vegetation condition. In summary, the combination of microwave remote sensing (active and passive) constitutes a good option, in which the best of both systems (high spatial resolution from SAR and high temporal resolution from passive systems) can be exploited for large river basins monitoring. This led us to the development of a methodology to retrieve flooded area in herbaceous wetlands, based on active/passive microwave data [3].

Currently there are several passive systems available, which present different characteristics (resolutions, frequencies, and incidence angles). In this study, we analyze the multi-frequency temporal trends of available radiometers (Aquarius (L Band), SMOS (L Band) and AMSR2 (C, X, Ka Band)) to estimate the fraction of flooded area inside a wetland floodplain. The influence of resolution, frequency and incidence angles are discussed using model simulations. In this case Cosmo Skymed data acquired once every ~20 days is used to compute high resolution flooding maps that are used to recalibrate the parameters (mainly the Polarization difference of flooded area) in order to enhance the accuracy of passive data flooded area fraction estimation performed with a temporal resolution of a few days to a week.

The Paraná River Delta was selected as test site. In April-June, 2013, strong rains fell over the upper Paraná Basin (South of Brazil and North-East of Argentina), leading to the occurrence of a moderate flood wave that reached the lower

Paraná Basin (including Paraná River Delta) on July, 2013. In this context, the objective of this paper is to estimate flooded area fraction from passive microwave data. The general approach is based on the exploitation of the PI from a complete series of passive data, and the use of high resolution flooding maps based on Cosmo Skymed data in specific dates for parameter calibration [3]. We show the feasibility to monitor flood condition with the combination of active and passive microwave data, and the effects of spatial resolution, frequency and incidence angle of passive data in the algorithm performance.

II. MATERIALS AND METHODS

A. Paraná River sub-basin and Paraná River Delta

The lower part of Paraná River is subject to strong variations of water level, related to local rain events and the contribution of up-water of Paraná and Paraguay Rivers.

In this paper, we studied the area shown in Fig. 1. It encompasses the Paraná River floodplain, which is topographically lower than its surrounding areas and is covered by a highly heterogeneous wetland with a complex landscape pattern. Nevertheless, at the spatial scale of AMSR-E, this wetland is dominated by lagoons and different communities of herbaceous vegetation in the extended lowlands.

In April-June, 2013, strong rains fell over the upper Paraná Basin (South of Brazil and North-East of Argentina), leading to the occurrence of a moderate flood wave that reached the lower Paraná Basin (including Paraná River Delta) on July, 2013 (Fig. 2).

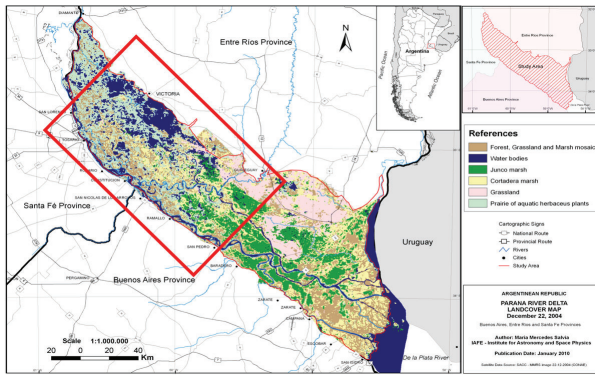


Fig. 1. Paraná River Delta. The studied area is shown in red.

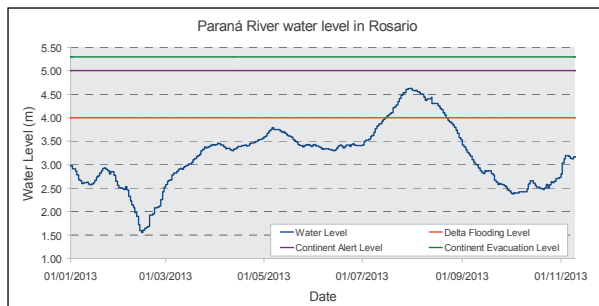


Fig. 2. Paraná River water level in Rosario Port.

B. Instruments and datasets

To estimate the hydrological condition of this area, we used both active and passive microwave signatures, as well as ancillary data. In particular, we used Cosmo Skymed ScanSAR Wide data and brightness temperature from AMSR2, SMOS and Aquarius/SACD. Details about product characteristics are given in Table I.

C. The algorithm

Basically, the passive data have been analyzed using the simple model proposed by [1]. The model has three end-members, that represent the contributions of water, non-flooded land, and inundated floodplain to the total observed polarization index PI_{obs} ,

$$PI_{obs} = f_w PI_w + f_{nf} PI_{nf} + f_f PI_f \quad (1)$$

$$1 = f_f + f_{nf} + f_w \quad (2)$$

where PI_{obs} is the PI observed by the radiometer, f_w , f_{nf} and f_f are the fractional areas of open water (rivers and lakes without emergent vegetation), non-flooded land, and seasonally flooded land, respectively, and PI_w , PI_{nf} , and PI_f are the PI values for open water, non-flooded land, and seasonally flooded land.

The algorithm is based on the following hypothesis:

1. The polarization index of water bodies, PI_w , is constant and known (emission model simulations).
2. The fractional area of permanent water bodies is constant and known (land cover map).
3. The polarization index of non-flooded land, PI_{nf} , is constant, shows a unique value for all the non-flooded vegetation types present in the area and can be estimated, in our case from emission models (emission model simulations).
4. The polarization index of flooded land, PI_f , is constant, shows a unique value for all the flooded vegetation types present in the area, has a negligible dependence on flood condition and can be estimated from images. The estimation of this value is a critical part of the algorithm and presents large variations as reported in [1].

TABLE I. USED PRODUCT CHARACTERISTICS.

Sensor	Data used	Dates	Variable obtained
Aquarius (L Band)	L2 V2 Tb	2013/05-2013/11	$PI = \frac{2(Tb_v - Tb_H)}{(Tb_v + Tb_H)}$
SMOS (L Band)	SCLFIC Tb	2013/05- 2013/11	PI (35 to 45° average)
AMSR2 (C, X and Ka Bands)	L1B Tb	2013/05- 2013/11	PI
Cosmo Skymed ScanSAR Wide (X Band)	HH σ^0	2013/07/05, 2013/07/25 2013/08/10, 2013/08/30 2013/09/15, 2013/10/08 2013/10/20, 2013/11/05	Flooded area maps [4]
Emission model	Ferrazzoli and Guerriero, 1996 [5]		
Auxiliary data	Water level in Rosario Port, Land Cover map [4]		

Previous work [6] has proven hypothesis 4 not to be valid for our study area, since the increase of water level reduces the height of the vegetation, causing a decrease in emission but an increase in PI.

Since PI_f is one of the key parameters of our algorithm, Cosmo Skymed images were used in conjunction with passive microwave data to estimate PI_f at regular basis. Basically we obtained higher resolution flooding maps by thresholding a change image constructed via image algebra of Cosmo Skymed images at regular intervals. We calculate f_f for our study area from those maps, and use it to estimate PI_f from nearly coincident passive images.

In order to retrieve fraction of flooded area for the whole temporal series of passive microwave data we need to obtain PI_f for passive images in the period between two consecutive Cosmo images. For this, a linear interpolation scheme was used, since it is the simpler method that requires less assumptions.

In addition, for dates with both passive and active microwave data availability, we estimated floodplain water level using the PI_f estimated using both active and passive microwave images and the emission model simulation results.

The proposed algorithm and the data source of each involved parameter are shown in fig. 3.

III. RESULTS AND DISCUSSION

For each of the passive microwave system used we analyzed the temporal behavior of observed PI in comparison with Cosmo Skymed derived flood area fraction, and hydrometric river water level measured at Rosario port (fig. 4).

Fig. 4 upper plot shows that AMSR2 observed PI has a good agreement with flooded area fraction estimations from Cosmo Skymed higher resolution SAR images, and both of them follow the trend of river water level, with a lag of approximately 10 to 15 days. This could mean that Rosario may be the point of entrance of water to the floodplain, and the lag is the time it takes the water to be distributed throughout the floodplain.

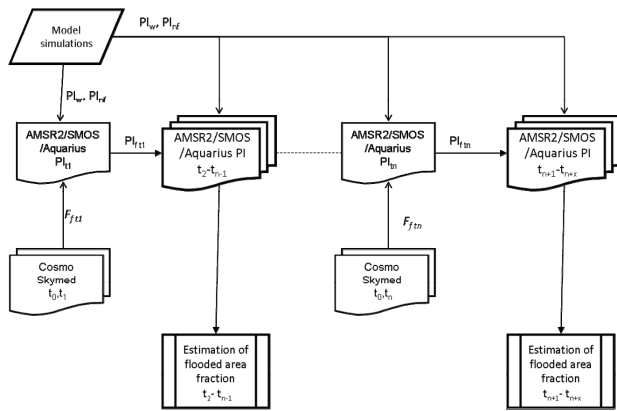


Fig. 3. Flowchart of proposed algorithm

It can also be seen that Ka band is noisier than X and C bands, which could be related to atmospheric noise like rain clouds, that affects Ka band (36.5 GHz) but has almost no effect at X (10.7 GHz) and C (6.9 GHz) bands.

Fig.4 center plot shows that even though SMOS data are much noisier than AMSR2 data, we can still see some agreement between PI and flooded area fraction estimated from Cosmo Skymed data, especially in the case of Ascending passes of SMOS. Descending passes are noisier than ascending passes, although this could be an effect of the different amount of available data (48 acquisition for ascending and 83 for descending passes). The fact that overall SMOS data are noisier than AMSRE could be due to some residual RFI (Radio Frequency Interference), since the studied area is adjacent to Rosario city, which is the 3rd largest city of Argentina. Given that we had more data from descending than from ascending passes, we decided to use for flooded area fraction retrieval only the descending passes.

Fig. 4 lower plot shows that Aquarius observed PI has low sensitivity to flooded area fraction from Cosmo Skymed data. This could be due to the large footprint size (100 km diameter footprint at -3dB), that causes observed PI from footprints used to include a range of continent/wetland area ratio.

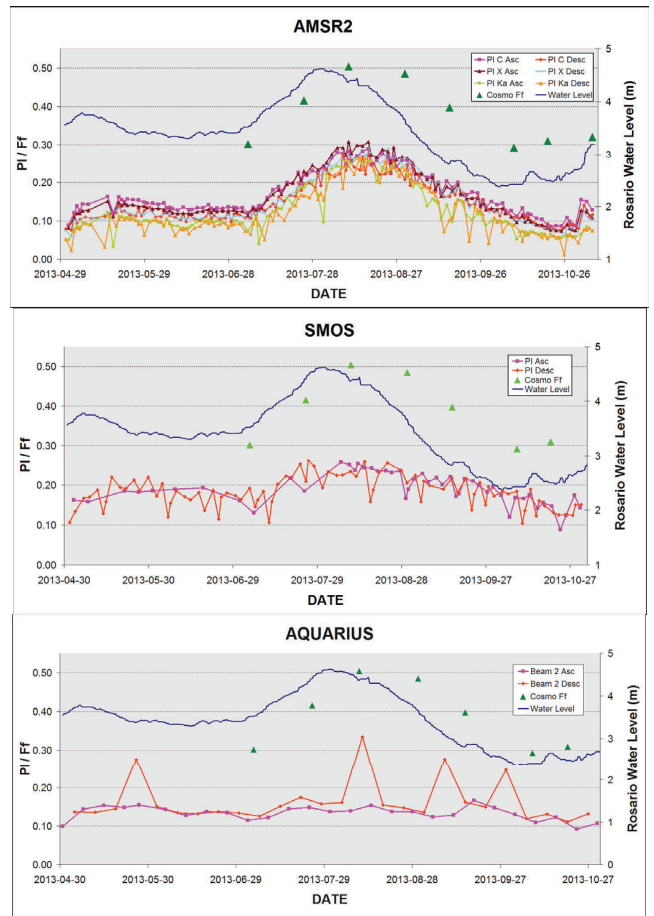


Fig. 4. Observed PI, Cosmo Skymed derived f_f and river water level in Rosario port. Upper: AMSR2. Center: SMOS. Lower: Aquarius.

Descending passes are noisier than ascending passes, showing peaks at regular intervals that could not be explained from the bio-geophysical point of view. According to this, for flooded area fraction retrieval we used only Aquarius ascending passes.

Fig. 5 shows the results of the emission model for each of the frequencies used (L, C, X and Ka bands). These simulations were used to obtain the values of PI_{nf} and PI_w . For each band, values of PI obtained for WL = 0 and WL = 180 were used respectively. Simulation where obtained using the procedure described in [3]. Fig. 6 shows estimated PI_f for dates with Cosmo Skymed data availability, and the linear interpolation used for periods between 2 consecutive Cosmo images.

Estimated and interpolated PI_f show good agreement for C and X bands of AMSR2, as well as between ascending and descending passes but Ka band estimations show differences on this trend from September on. This could be due to the fact that Ka band observed PI is much noisier than C and X band data. In the case of Aquarius, PI_f shows a decrease in the dates of higher Cosmo f_f instead of the expected increase. This could be due to the low sensitivity of PI_{obs} to the event because of its large footprint size, as explained previously. In the case of SMOS, PI_f shows a strong increase at the beginning of the event (for date 2013-07-25), but then PI_f decreases to previous values, showing low sensitivity to the progression of the event.

Fig. 7 shows the fraction of flooded area obtained using the proposed algorithm. AMSR2 derived f_f shows good agreement with Cosmo f_f from July to September. Much noisier estimations previous to July could be due to the extrapolation of PI_f obtained for early July to previous dates. Estimated values from September on do not follow the trend of Cosmo derived f_f , showing that the linear interpolation scheme of PI_f , although correct from the point of view of the inference, could be an oversimplification. Given the fact that observed PI for Ka band was much noisier than PI_{obs} for X and C band, derived f_f for Ka band are much noisier than those for X and C band.

SMOS derived f_f shows a similar trend to the described for AMSR2, but is much noisier than C and X band estimations all over the study period (and noisier than Ka band estimations for the rising period), as was expected from noisier observed PI with lower sensitivity to flooding and from PI_f values shown on fig. 6 and discussed previously.

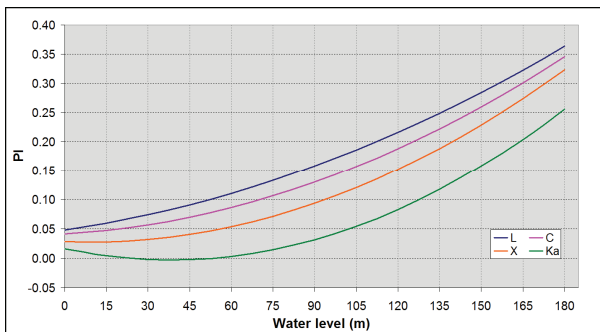


Fig. 5. Emission model results.

Aquarius derived f_f shows lower values along the whole flooding period, they show some agreement with Cosmo derived f_f at the beginning of the event, but they diverge after the flooding peak (end of August). This is consistent with the poor agreement found in the observed PI and PI_f shown on fig. 4 and 6, and has been explained previously.

Fig. 8 shows estimated water level using PI_f from fig. 5 and model simulations from fig. 6. It can be seen that for AMSR2 there is a smaller dynamic range of the estimations as compared to f_f , which is consistent with the fact that PI_f from that system show a similar trend. Aquarius estimated WL show a different trend which is consistent with its PI_f , showing a decrease instead of the expected increase with the progression of the event. SMOS WL also shows the same trend than PI_f , but the peak that was observed in PI_f is not present in WL. This is because there is a saturation point at a WL of 1.8 m due to the fact that at that level, water completely covers vegetation, and $PI_f = PI_w$. From this point on, an increase in water level does not cause an increase either in PI_f or in PI_{obs} .

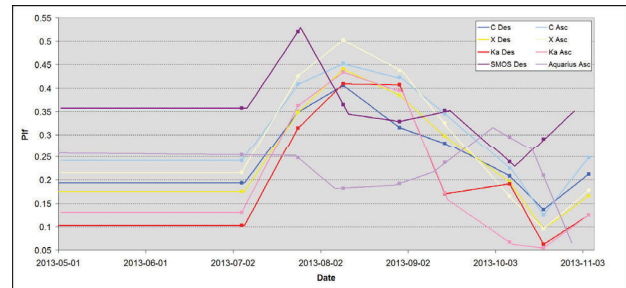


Fig. 6. Linear interpolation of estimated PI_f (lines). PI_f for dates of Cosmo f_f availability are marked with square

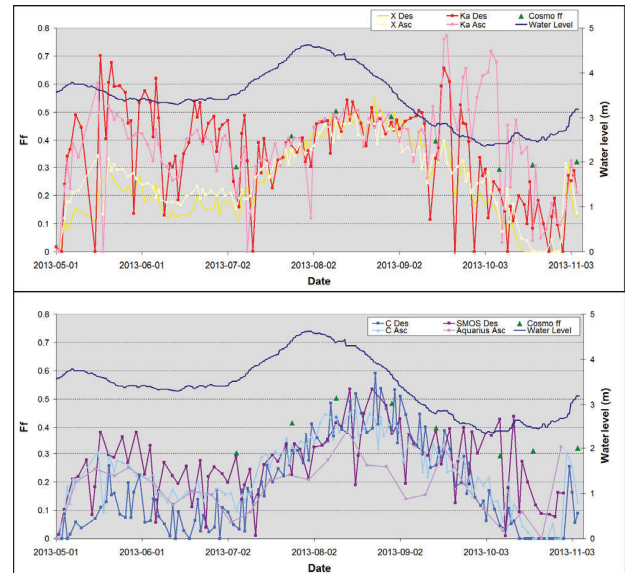


Fig. 7. Estimated fraction of flooded area (f_f) for AMSR2 (Ka, X and C bands), SMOS (Lband) and Aquarius (Lband). Cosmo based f_f and Paran River water level are shown for comparison.

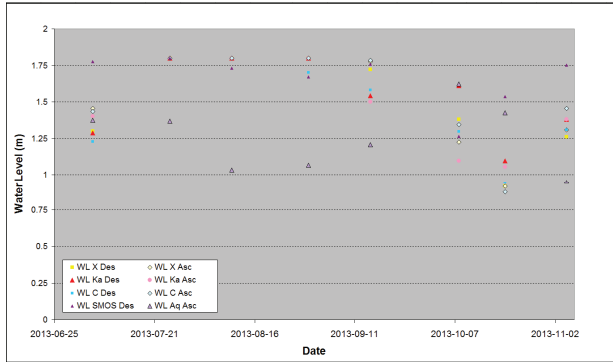


Fig. 8. Estimated water level for AMSR2 (Ka, X and C bands), SMOS (Lband) and Aquarius (Lband). Paraná River water level is shown for comparison.

IV. CONCLUSIONS AND FUTURE WORK

The expected result in case of a robust algorithm would be a consistent estimation of flooded area fraction among all sensors and frequencies available. The proposed algorithm was close to that goal for the rising period of the event, especially for AMSR2 data. However, further work is needed in the low waters period and on the falling stage of the event, since estimated ff values deviate from those obtained with Cosmo Skymed higher resolution SAR images.

Even though we think the general scheme is correct, some improvements are needed in the following issues:

- A more refined interpolation method is needed for PI_f , in order to improve ff estimations in the low waters period and falling stage of the event.
- A more detailed preprocessing might be needed for SMOS data to better avoid RFI induced noise.
- Given the large footprint of Aquarius, a preprocessing scheme to eliminate continental influence in a footprint basis is needed.
- Future work will also include the use of distributions for the simulations and algorithm input parameters instead of their mean values.

Finally, it is important to remark that the simulations show that L band PI should be more sensitive than Ka band PI to changes in water level for low water levels. This should have important consequences for the retrieval.

In the scheme proposed by [1], the three components assumption (i.e. flooded, non-flooded, permanently flooded) were justified because Ka band data were used, for which small

changes in water level for low water level conditions produce a negligible effect on observed brightness temperatures (T_b), and thus on PI. Therefore, a change in PI at Ka band will be related only to a change in flooded fraction (where flooded is considered when the vegetation is completely covered by water). On the contrary, it is expected that even a small increase in water level or partial flooded fraction would produce an increase in the observed PI at L band (see figure 5). This is another reason (besides pixel size and RFI), which probably conditions L band flooded fraction retrievals within the three components scheme, that even if using high resolution L band systems (e.g. SMAP), will probably require the inclusion of additional terms.

ACKNOWLEDGMENT

The authors specially thank the National Commission for Space Activities (CONAE) for the provision of Cosmo Skymed data, the European Space Agency (ESA) for SMOS data, National Aeronautics and Space Administration (NASA) for Aquarius data, and Japan Aerospace Exploration Agency (JAXA) for AMSR2 data. Hydrological data were provided by Prefectura Naval Argentina.

REFERENCES

- [1] Sippel, S.K., Hamilton, S.K., Melack, J.M., and Choudhury, B. "Determination of inundation area in the Amazon River floodplain using the SMMR 37 GHz polarization difference". *Remote Sensing Environment*, 48: 70-76, 1994.
- [2] Prigent, C., F. Papa, F. Aires, W. B. Rossow, and E. Matthews, "Global inundation dynamics inferred from multiple satellite observations, 1993–2000", *J. Geophys. Res.*, 112, D12107, doi:10.1029/2006JD007847. 2007.
- [3] Salvia, M., Grings, F., Ferrazzoli, P., Barraza, V., Douna, V., Perna, P., Brusantini, C., Karszenbaum, H. "Estimating flooded area and mean water level using active and passive microwaves: the example of Paraná River Delta floodplain". *Hydrol. Earth Syst. Sci.*, vol. 15, 2679–2692, 2011.
- [4] M. Salvia, H Karszenbaum, P. Kandus and F. Grings "Datos satelitales ópticos y de radar para el mapeo de ambientes en macrosistemas de humedal", *Revista de Teledetección*, vol. 31, 35-51, 2009.
- [5] Ferrazzoli, P. and L. Guerriero, "Emissivity of vegetation: theory and computational aspects", *J. Electromagnet. Wave.*, vol. 10 (5), 609-628, 1996.
- [6] Salvia, M., Grings, F., Perna, P., Ferrazzoli, P., Rahmoune, R., Barber, M., Douna, V., Karszenbaum, H. *Monitoring flooded area fraction in floodplains of Paraná basin using passive and active microwave systems*. 2010. *International Geoscience and Remote Sensing Symposium (IGARSS) 2010*.